

CHAPTER II

THE EXPERIMENTAL SET UP

2.1. Introduction

In this investigation experimental observation and theoretical interpretation of the optical and electrical properties of arc plasma both in absence and in presence of either transverse or longitudinal magnetic field has been performed. In this scheme the plasma parameters of the discharge (not always of positive column) have been measured using different techniques. In our investigation low pressure mercury arc and metal arcs in air with four different types of electrodes (a) Silver-Silver, (b) Copper-Copper, (c) Iron-Iron and (d) Silver-Copper (in this case silver is the anode and copper is the cathode) have been used as plasma sources.

As in low pressure discharge the mean free times of the plasma species are large, plasma transport properties will be more influenced by the magnetic field and therefore, a low pressure plasma with a low input energy has been taken to study the effect of magnetic field in particular. The magnetic field is either axial or perpendicular to the main discharge current. In case of low pressure mercury arc, before any set of observations is made, a steady state of the discharge has first been obtained; thereafter the plasma parameters under interest have been studied.

2.2. Arc tube

All arc tubes in which experiments have been carried out are made of pyrex glass. For low pressure mercury arcs, the arcs have been produced between two mercury pool electrodes (fitted with two tungsten wires for external electrical connections) by a 250 volt d.c. source from a d.c. generator. All the arc tubes have been designed and constructed in the laboratory (Fig. 2.1). They are fitted to simple traps in such a way that the mercury vapour coming out of the tube would condense easily and return to the tube. Otherwise, mercury would condense in the connecting rubber tubes and a mercury plug would be formed in the passage of air and would thereby disturb the vacuum arrangement. The whole arc system is cooled down by air coolers and two mercury pool electrodes by circulation of water.

2.3. Cleaning procedure of the arc tube

As a preparation for constructing mercury arc the glass tube was thoroughly washed with dilute chromic acid and then with NaOH solution. The discharge tube was then washed several times with distilled water and then with dehydrated pure benzene. Then the tubes were heat backed in an electrical oven. Triple distilled mercury was then introduced into the tube to the desired quantity. The tube was then connected to a double stage rotary vacuum pump and a vacuum of the order of 10^{-2} torr, was obtained.

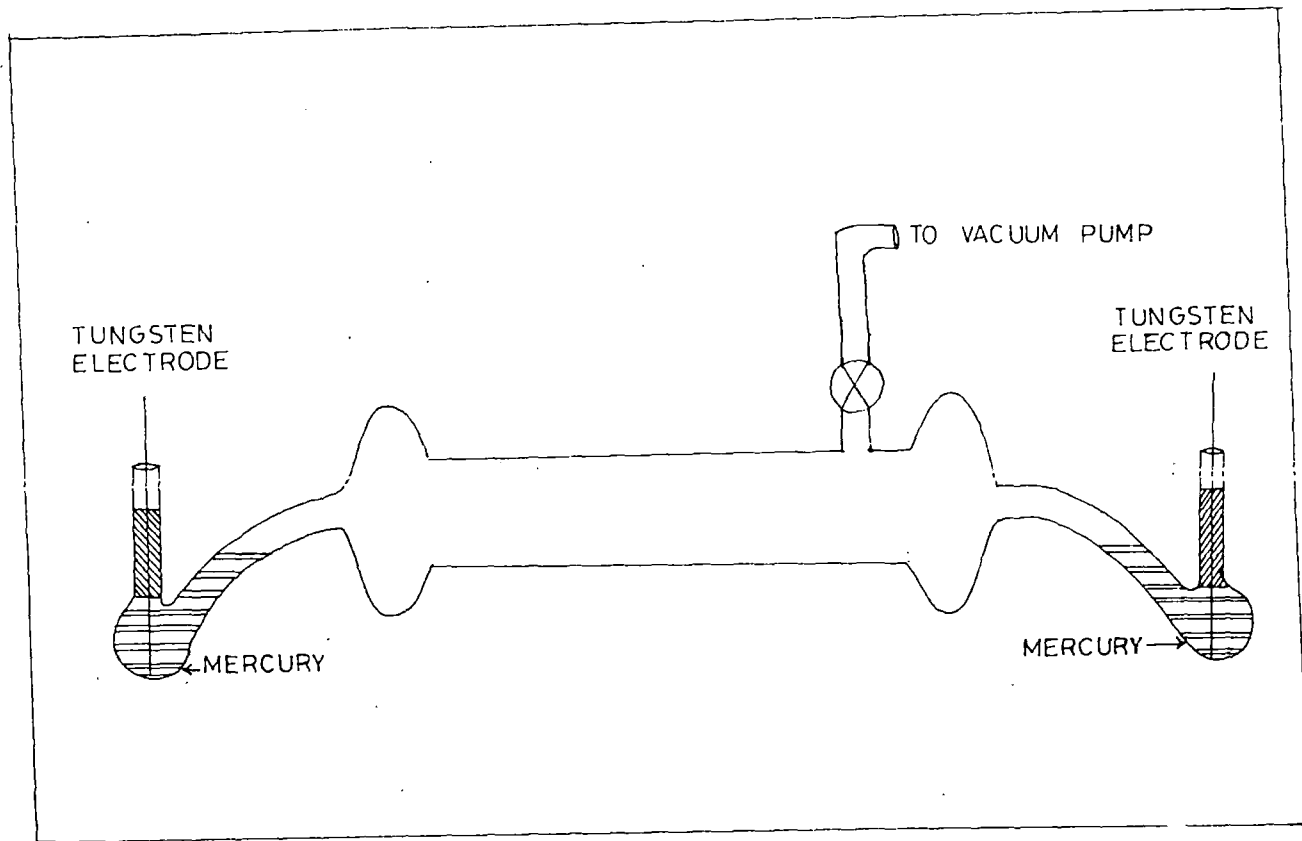


FIG. 2.1

DIAGRAM OF A MERCURY ARC TUBE.

2.4. Procedure for pressure measurement

A pirani gauge has been used in the arc tube line and through it the pressure of background dry air (buffer gas) has been measured. A needle valve has been placed in the arc tube line to allow a micro-leak for adjustment of air pressure inside the system.

The pressure of mercury vapour has been measured from standard tables (Hodgman, 1956) after calculating inside wall temperature T_w of the tube which is equal to the outside wall temperature increased by the temperature drop over the tube wall resulting from the cost of energy which is dissipated in the tube and carried away via the tube wall (Verweij, 1960). The outside wall temperature has been measured by a mercury in glass thermometer when the arc exists in a steady state condition. In the experiments the arcs have been cooled down by air coolers. Therefore, a steady outerwall temperature corresponds to a steady condition of the arc under investigation. After Verweij (1960) the temperature drop has been estimated by considering that the total energy dissipated $W = Ei$ per cm along the tube length. Here E is the magnitude of electric field measured by noting the voltage drop across the arc minus standard cathod fall of 10 volts as measured by Lamar and Compton (1931), then divided by the entire arc length and i is the arc current. In fact, the amount of energy which escapes as radiation through the tube wall is comparatively small and the ultraviolet resonance radiation is absorbed within a very

small penetrating depth in pyrex glass wall of the arc tube. Therefore, the dissipated energy flux is carried away mainly by thermal conduction through the surface area of 1 cm. of the arc tube length, hence through $2\pi R$ sq.cm. (R is the inner tube radius). The temperature drop ΔT_w is given by

$$W = 2\pi R K \frac{\Delta T_w}{d} \quad (2.1)$$

where K is the thermal conductivity of the glass (K pyrex 11×10^{-3} joule/cm/sec/ $^{\circ}$ C) and d is the thickness of glass wall. For a typical operation of arc at a current of 3.0 A, ΔT_w has amounted to 7 - 8 $^{\circ}$ C. A plot of saturated vapour pressure of mercury (P_{Hg}) with T_w has been shown in Fig. (2.2). As number density of ground state mercury atoms N_g is explicitly related with P_{Hg} by the relation

$$N_g = 3.3 \times 10^{16} \frac{P_{Hg}}{T_w} \quad (2.2)$$

N_g has also been plotted against T_w in the Fig. (2.2)

2.5. Magnets and power supplies

The magnetic field has been provided by electromagnets. Depending upon the lengths and diameters of the arc tube, gap between the pole pieces of electromagnets has been adjusted. For accuracy in measurement, the pole pieces have been so chosen that the magnetic field was uniform and without having

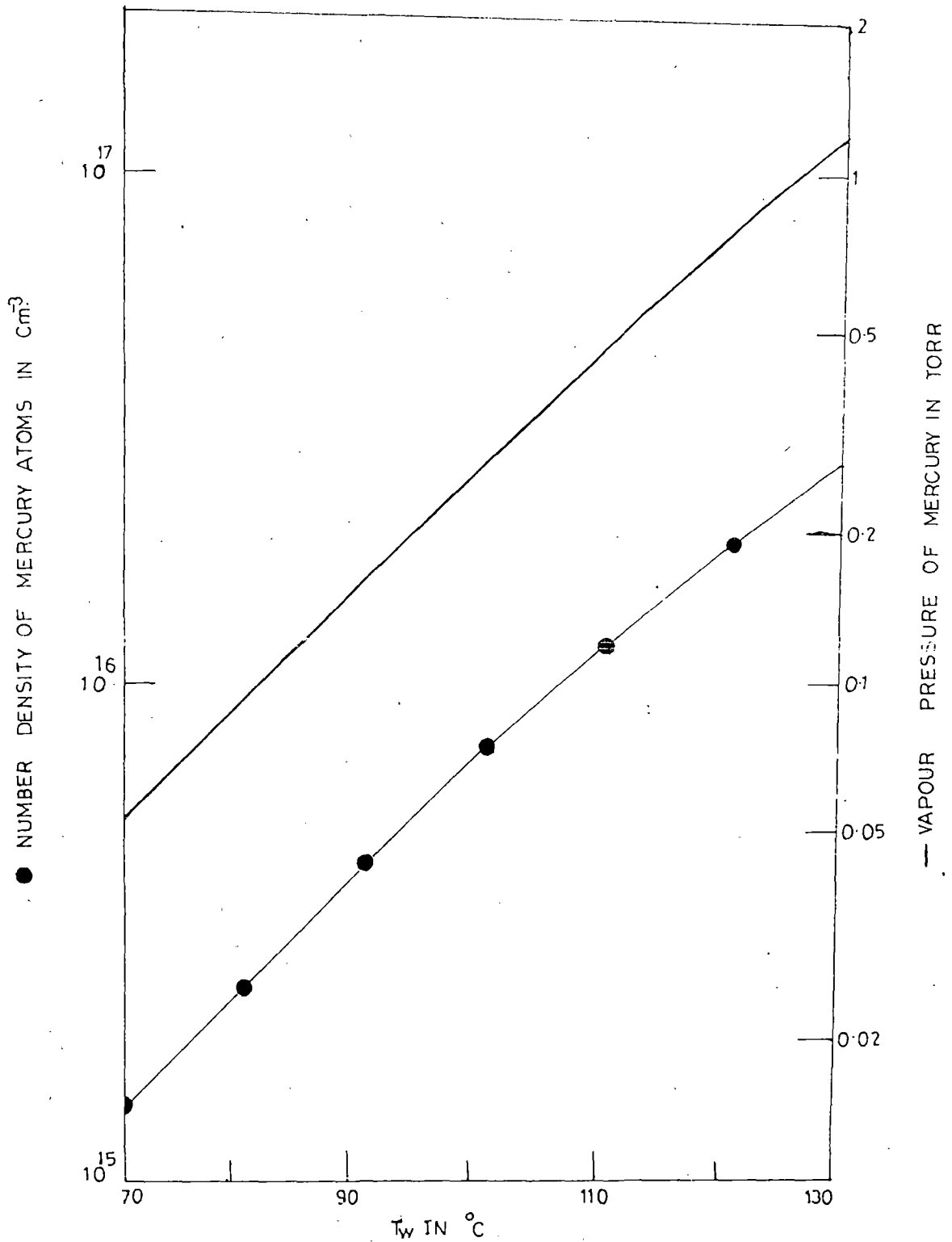


Fig. 2.2. Variation of vapour pressure and number density of mercury atoms with temperature of outer wall (T_w) of discharge tube.

any radial magnetic field component. For investigation in longitudinal magnetic field, the total arc tube has been placed in between the pole pieces as shown in Fig. (2.3), when a transverse magnetic field is utilised only certain portion of the positive column of the arc tube where investigations have been made, has been inserted in between the pole pieces Fig. (2.4).

The magnetic field strength has been measured by gauss meter (Model G14). The electromagnets have been run by a stabilised d.c. power supply (Type EM20).

Both the mercury arc in the tube and some other metal arcs (in air) using Ag-Ag, Cu-Cu, Fe-Fe and Ag-Cu electrodes have been produced by a d.c. generator whose voltage may be adjusted by a rotary variable resistor fitted externally (in the front panel of a steel stand) and current can be adjusted with a rheostat inserted in series with the electrodes. The arc current has been varied upto 5A. For photo multiplier tube, oscillator and d.c. amplifier the power supplies have been fabricated in the laboratory. The circuits for their fabrication have been taken from Radio Amateur's Handbook (1965).

The calibration curves for the magnetic field for different settings have been shown in Fig. (2.5), (2.6), (2.7) and (2.8) respectively.

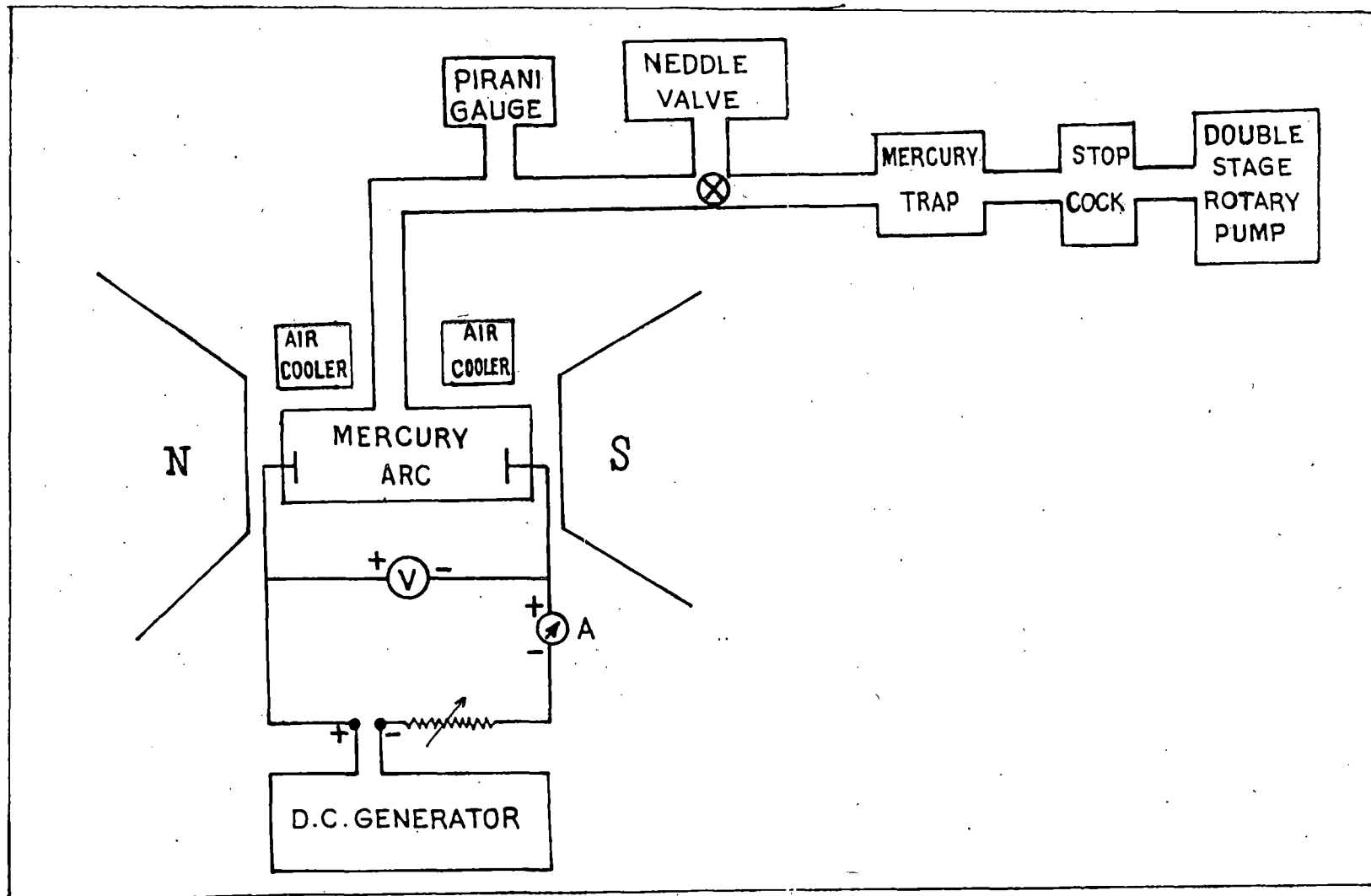


Fig. 2-3. Schematic diagram of experimental set-up in an axial magnetic field.

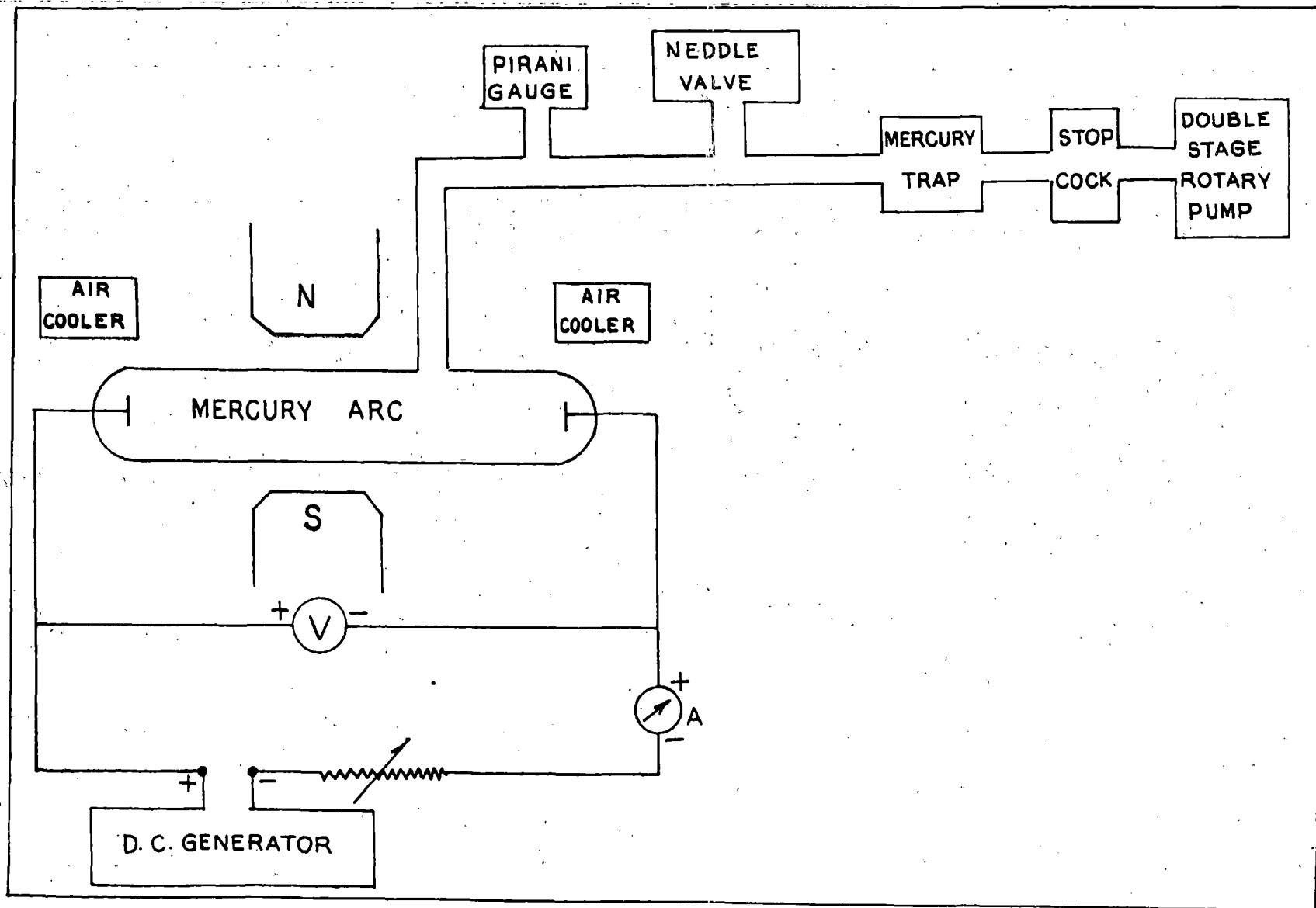


Fig. 2.4. Schematic diagram of experimental set-up in a transverse magnetic field.

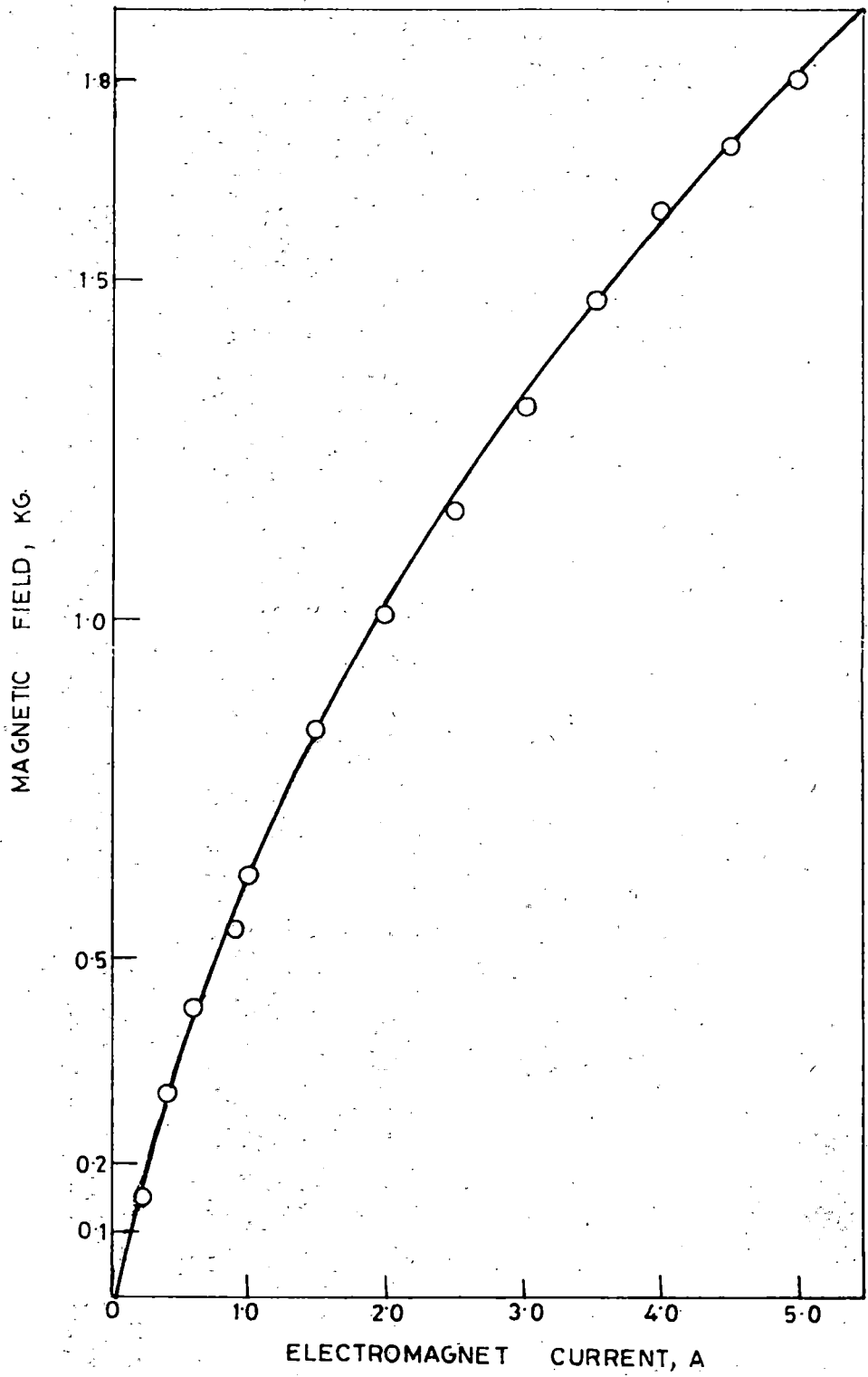


FIG 2-5. MAGNETIC FIELD CALIBRATION CURVE. Ref. chap. III

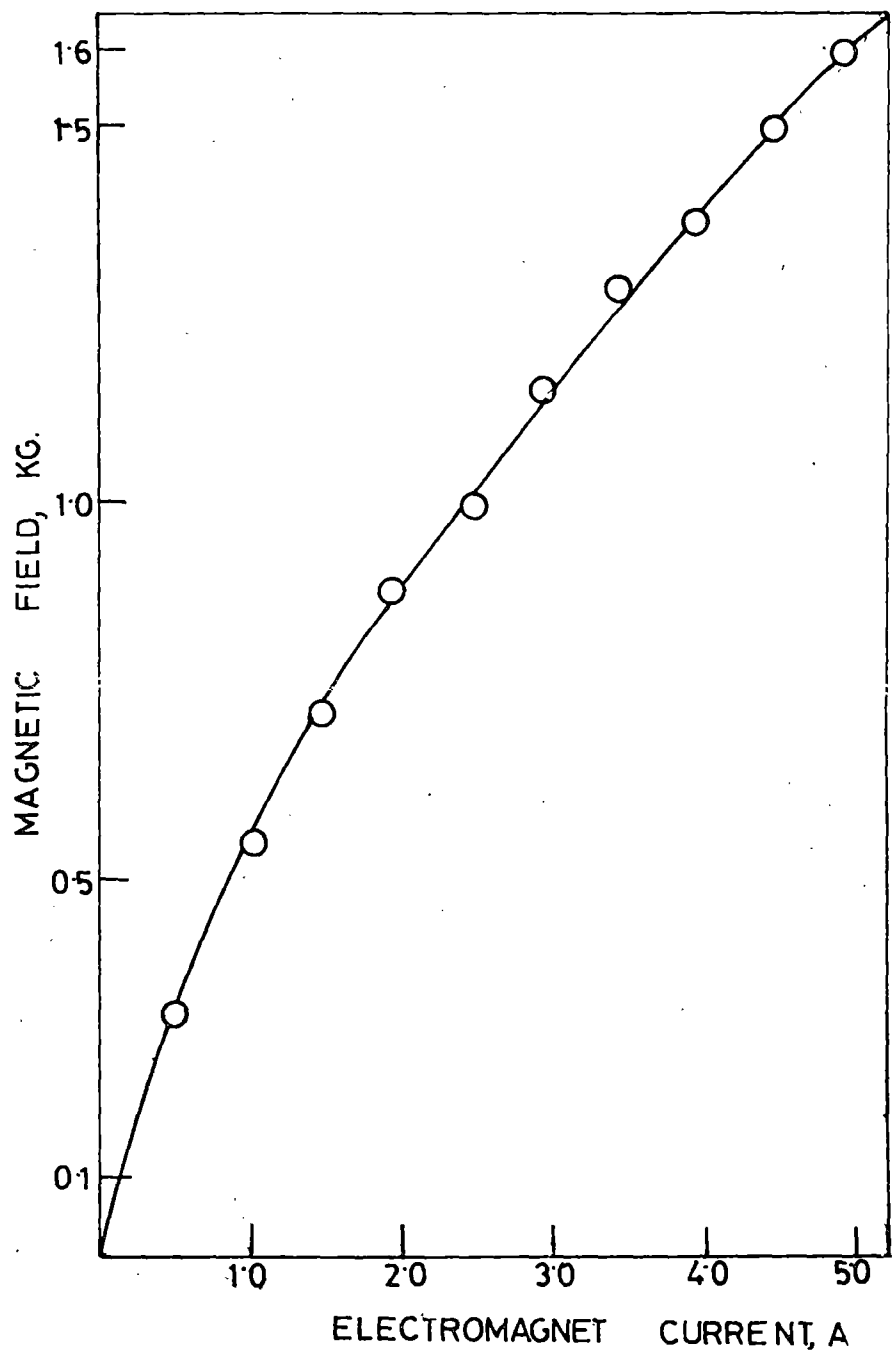


FIG.26.MAGNETIC FIELD CALIBRATION CURVE
Ref. Chap, IV.

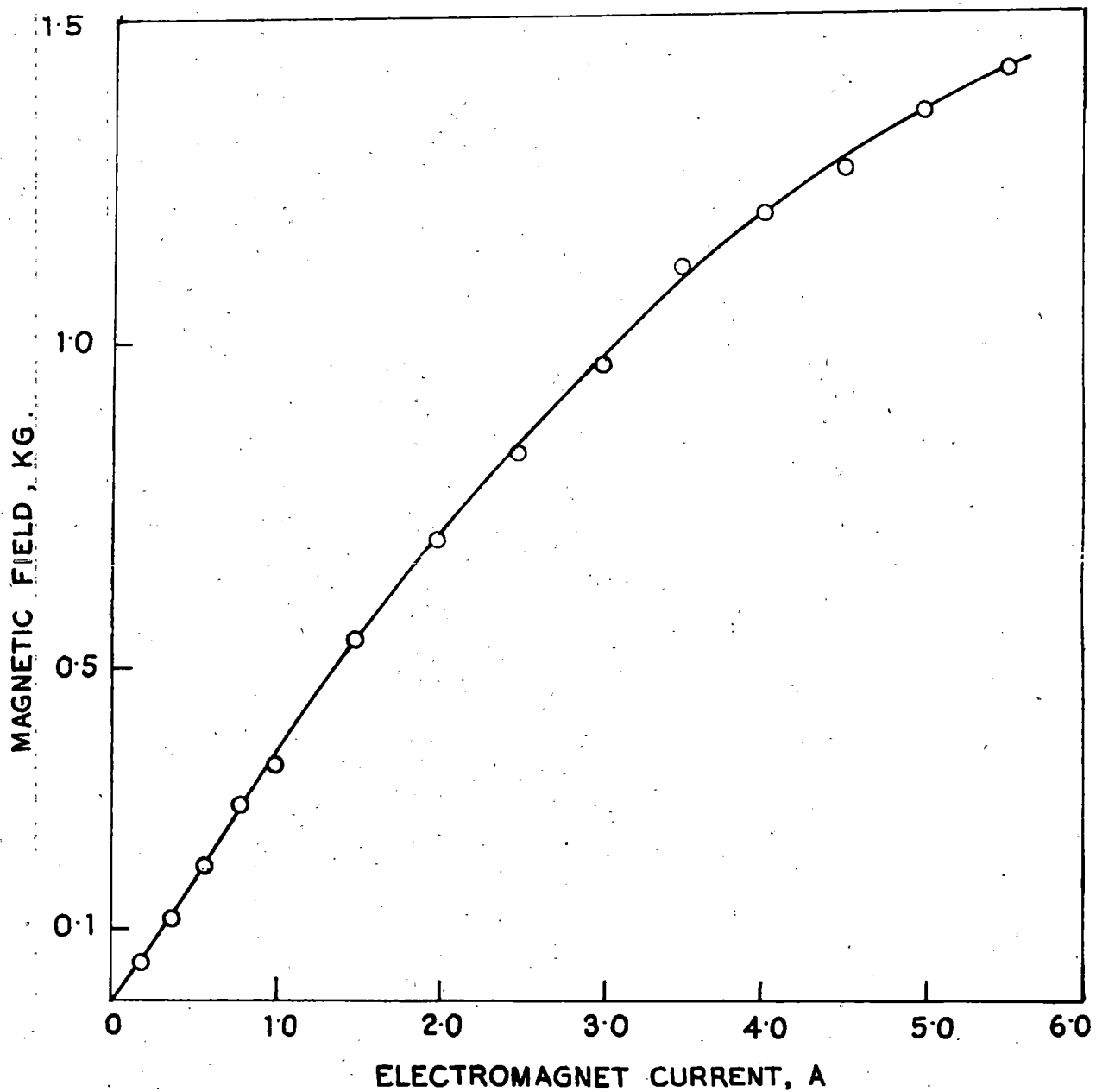


Fig. 2-7. Magnetic field calibration curve , Ref. chap.V.

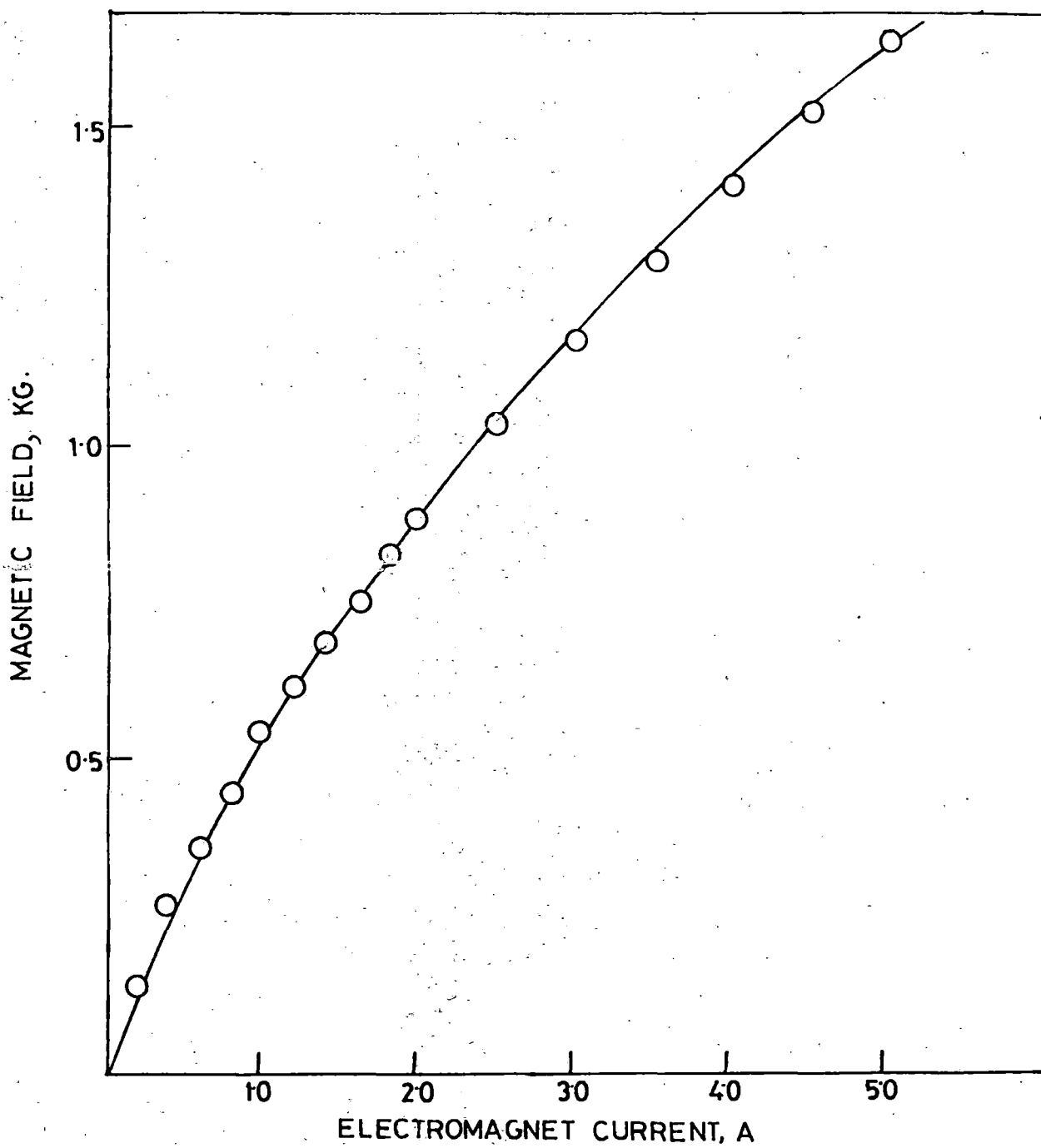


FIG-28. MAGNETIC FIELD CALIBRATION CURVE ; Ref. Chap. VII.

2.6. Spectroscopic measurements

Spectroscopic diagnostic method has been adopted to estimate plasma parameters in transverse magnetic fields. In the investigations the experimental set up used has been drawn in Fig. (2.9). The visible radiations from the axial part of the arc tube placed in between the pole - pieces of the magnet enters through a vertical slit and and is focussed by a double convex lens fitted on the vertical slit of the collimator of the constant deviation spectrograph. In this spectrograph, there is a Pellin-Broca prism for 90 degree deflection of the spectrum. Such a mounting is necessary as the monochromator is with fixed slit. The exit slit is perpendicular to the plasma source. The wavelength of the source (arc spectral lines) is changed by rotating the prism with a mechanical arrangement which is mounted with an accurately calibrated drum. The wavelengths of the visible spectrum have further been checked from standard values given in Handbook of Chemistry and Physics [Hogman (1956)]

This type of apparatus has a low resolving power which would be advantageous in the present investigations because it is unable to resolve Zeeman splitting. The slit width can be adjusted with ^{the} help of a micrometer arrangement from 0.25 mm to 1 mm depending on the response of spectral lines focussed to the photomultiplier tube. For a set of observation however, the slit width has been kept fixed.

The collimator is focussed by rack and pinion arrangements; the selected spectral line has been focussed on the cathode of the photomultiplier tube MIOPS29V_λ operated at 1425V. The top-cathode type photomultiplier which has low mean radiation equivalence of dark current is placed in a darkened ebonite housing behind the eye piece of the spectrograph. The power source of photomultiplier is provided in two sections: the first is 1200 V stabilised to supply the dynode voltage and the second is to provide 225 V between the final dynode and the anode (Fig. 2.10). The second voltage source is also used to operate the V.T.V.M. It consists of two 6J7 tubes operated at 32V on the plates and 1.3V negative grid bias. The grids are connected to the two ends of a resistor R_1 (600 K Ω) which is in series with the plate of the photomultiplier. In operation, when current flows through the resistor R_1 , a potential drop developed and one of the 6J7 tubes draws less current producing an imbalance in the plate circuit. For this imbalance current measurement, a 0-200 μA meter is connected in between the plates of the 6J7 tubes. For this circuit arrangement, for a signal of 3V, the 6J7 tubes reached cut-off and beyond which there is no further increase in the meter deflection.

A coarse balance is made with R_4 with no radiation on the photomultiplier tube and the microammeter is set to zero with R_2 . In this way the effect of dark current in actual measurement of radiation is completely minimised.

With 3V or a little more applied to resistor R_1 , the meter is set to full scale deflection with the help of another resistor R_3 . The microammeter at the output records the radiation of the spectral line under investigation. The slit of the spectrograph is varied in such a way that meter deflection corresponding to the spectral line with strongest response to the photomultiplier is in the full scale range of the meter.

However, the spectral response of the photomultiplier depends on wavelength of incident radiation as well as quantum efficiency of the cathode material (the effect of photomultiplier window material is also present). A characteristic of quantum efficiency of MIOFS29V $_{\lambda}$ against wavelengths is plotted taking the values from Carl Zeiss brochure No. 40-637-2, in Fig. (2.11). From this characteristics the cathode radiant sensitivity in amperes per watt corresponding to a radiation of wavelength λ (\AA) is calculated as

$$S_{cr} = \frac{Q\lambda}{12395 \times 100} \quad (2.3)$$

here Q is the percentage of quantum efficiency, From determined value of S_{cr} the relative spectral sensitivity for two lines is estimated, and the microammeter reading for total intensities of lines is corrected for relative spectral response of the photomultiplier. The emission coefficient (ϵ_{ν}) corresponding to a radiation with frequency ν is proportional to observed total intensity

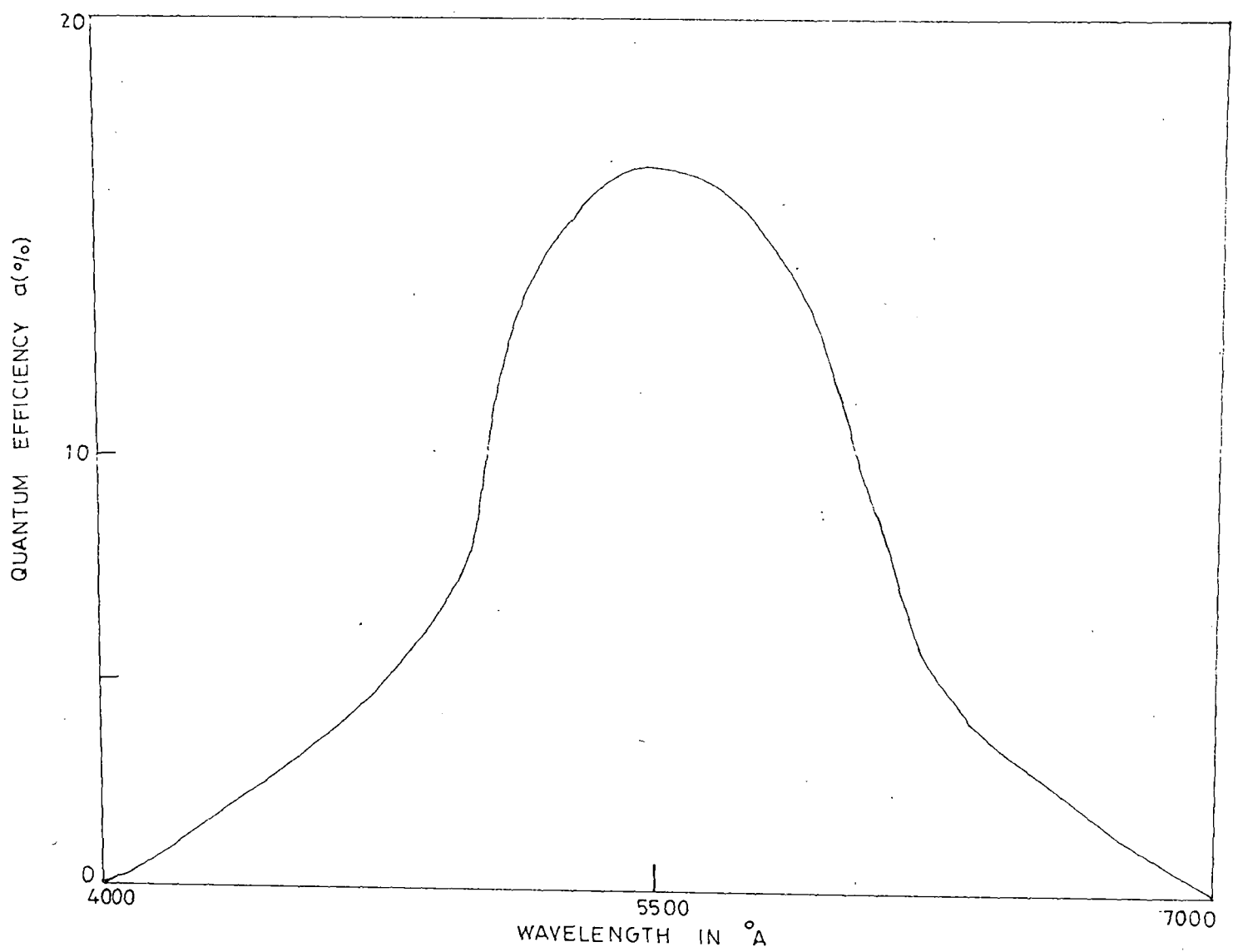


FIG. 2.11 QUANTUM EFFICIENCY IN % OF PHOTOMULTIPLIER M10F 529V_λ
(VEB CARL ZEISS JENA BROCHURE NO. 40-637-2.)

which is the sum of its continuous ($\epsilon_{\nu,c}$) and discrete ($\epsilon_{\nu,l}$) part. The discrete part contains the desired spontaneously emitted radiant energy within the line. In actual measurement the continuous part is eliminated by adjusting the resistor R_2 of the V.T.V.M. to the zero meter reading in the circuit focussing the continuum radiation at the vicinity on the photomultiplier tube cathode. Thus the microammeter current meter links only the line spectral radiation as contribution for the continuous part is negligible.

2.7. Procedure for persistence time measurement of afterglow in the mercury arc.

A Hartley oscillator has been utilised to provide radiofrequency voltage. A 6V6 vacuum tube is utilised as the oscillator. The output from the oscillator has been supplied to the arc through two coupled coils (one of the coils is wound around the tube) which with a variable gang condenser forms a secondary circuit (detector circuit). The r.m.s. amplitude of the oscillator output has been measured with the help of a half wave rectifier made of 6H6 tube inserted in parallel with the secondary tuned circuit. The applied radiofrequency voltage is tuned by the condenser when there is no arc discharge in the tube and the rectified output voltage is recorded by the D.C. voltmeter across a high resistance (in form of a resistive drop) which is in series with the rectifier tube. The level of radiofrequency

power supplied by the oscillator is low enough so as not to cause breakdown of the mercury vapour at the evacuated air pressure. The mercury arc has been produced in cylindrical arc tube by tilting processes. A pirani gauge has been kept always fixed with the system (as discussed earlier) to record the vacuum situation from time to time. To control the arc current several high current rheostats have been used in series with a d.c. ammeter (range 0 - 5A). During each set of observation the arc is run for a few minutes so that a steady condition is reached. It is worthwhile to note here that extreme precautions have been taken such that no element of the apparatus is disturbed during each set of observation. Then the primary arc has been switched off. Generally (without any other external field) afterglow vanishes immediately but due to superimposition of r.f. field, the afterglow persists and its persistence time has been recorded manually with the help of a stop watch with an error of ± 1 sec. very good care has also been taken during the whole observation, such that no mercury droplet would appear in the coil region, the presence of which changes the situation a lot. To observe the effect of magnetic field on persistence time of afterglow an electromagnet has been switched on as soon as the primary arc is switched off keeping other parameters unchanged.

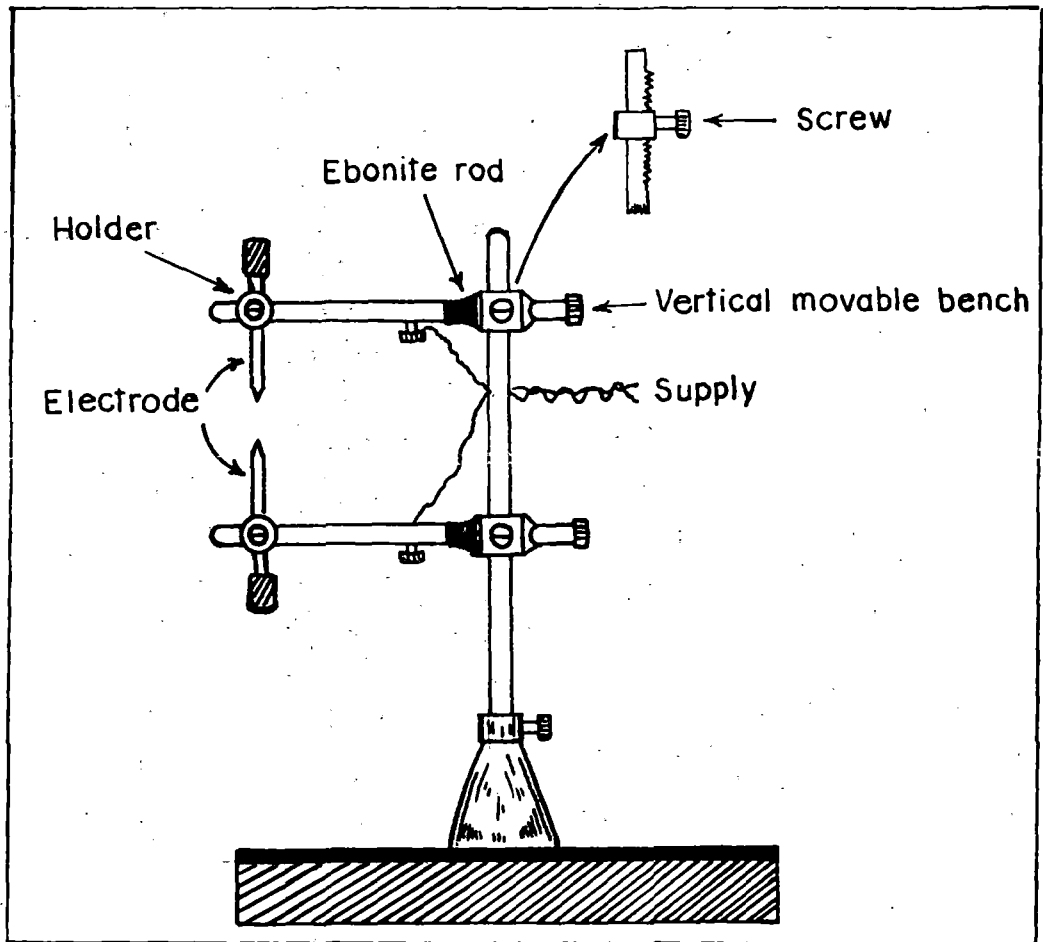
2.8. Measurement of voltage current and power relation in an arc plasma in a variable axial magnetic field.

Mercury arc is produced in a cylindrical glass tube. It's current is controlled by several high current rheostats. The current has been recorded by 0 - 5A meter. A V.T.V.M. of internal resistance $35M\Omega$ is utilised to measure the potential drop across the tungsten electrodes of the arc tube (Fig. 2.3.9), it is observed during the investigation that there is a slight fluctuation in arc voltage however, in the range of current and pressure used in this experiment, this process of fluctuation of voltage drop across the arc is very very small. However, Cobine (1958) explains this as due to continuous evaporation of cathode surface by heating. For evaporation of cathode, the length of the positive column slightly increases. Since the electric field in the positive column tries to remain unchanged, the voltage drop across the arc may show a slight change. The arc tube is horizontal and so designed that its mercury pools with external cooling arrangement condense the evaporated materials and return them to the bulk of the mercury. However, each set of measurement of voltage and current has been carried quickly enough so that the slower process of the time dependent effect as mentioned above may be ignored without losing accuracy. The variation of current and voltage for different values of magnetic field and different arc currents have been investigated.

2.9. Measurement of voltage current characteristics of low current arcs in air with metal electrodes.

Two respective metal electrodes of a particular arc have been fixed with a vertical stand as shown in Fig. (2.12) where upper metal electrode is attached to a vertically movable bench arrangement with the help of a screw. Initially the two electrodes were brought into contact by this screw. As it is a series element with a high current d.c. rectifier source (suitably filtered) and rheostats in series a desired amount of current flows through the electrodes. After the arc has been struck electrodes were separated gradually. A travelling microscope has been placed to measure the separation between the two electrodes after switching off current from the arcs (to avoid high intensity radiations). The voltage across the electrodes and current have been simultaneously measured with fixed and varying electrode separation. Before each set of observation the tips of the electrodes have been cleaned to avoid oxide coating and erosion. Special attention has been taken to record measurement as fast as possible and the whole system is allowed to run without any aircurrent (to make the arc quiet).

The diameter of the cross section of the tips of the electrodes before exciting the arc has been measured by the travelling microscope and then the arc has been run for usual measurements. The diameter of the electrodes was



METAL ARC ARRANGEMENT

Fig. 2:12

again measured when the electrodes cool down. Besides it, the tips of the electrodes were photographed and the diameter of the tips was obtained from measurements made with a travelling microscope. The last was necessary to estimate the cross section of the arc plasma.

2.10. Measurement of conductivity and power relation in an arc plasma in a transverse magnetic field

Two tungsten wires of diameter 0.28 mm within a glass capsule with bare tip of 0.1 cm have been introduced along the axis of the tube in the central portion of the tube length. A high impedance FET input meter has been utilised to measure conductivity (reciprocal of resistance) and the voltage drop between the two tungsten wires separated by 6.6 cm. The arc discharge current has been recorded by a 0 - 5 A d.c. meter. As discussed earlier, the voltage across the electrodes and current through the tube show a little temporal fluctuation. In this investigation, the voltage between the two probes immersed in the positive column does not effectively change with time because the entire bulk of the arc is not included in the measurement of the voltage (where cathode fall region and also anode fall region have been excluded). However, in the investigation, measurements have been taken repeatedly to avoid secondary time dependent effects. Measurements have been taken for a wide range of transverse magnetic field variation. After each set of observation the electromagnet has been demagnetised.

2.11. Measurements of electron temperature T_e and electron concentration in an arc plasma by probe method

A cylindrical metal probe (viz. tungsten) of 0.014 cm radius within a glass capsule with a bare tip of 0.1 cm length was inserted into the plasma at a distance of 14 cm from the anode (Fig. 2.13 a). The centre of the probe was fixed at the axis of the arc tube of 38 cm length and the probe was perpendicular to the axis. In common practice the length of the probe (l) should be greater than radius (r_p) of the probe. But an upper limit of the ratio l/r_p may be estimated from the expression of electron saturation current to the probe

$$I_{e(\text{sat})} = -n_e e A_p \left(\frac{T_e}{2\pi m} \right)^{1/2} \quad (2.4)$$

where m , e , n_e and T_e are the mass, charge, density and temperature of electrons and A_p is the probe collection area, $A_p = 2\pi r_p l$. It is preferable that $I_{e(\text{sat})}$ should not be too large so that probe would not become too hot (or incandescent) and gets damaged.

In the present investigation l/r_p was nearly 7.14. r_p and l were measured by a travelling microscope. It will be shown in chapter VIII that the results for the probe of these characteristic dimensions in arc plasma can be interpreted according to orbital motion theory.

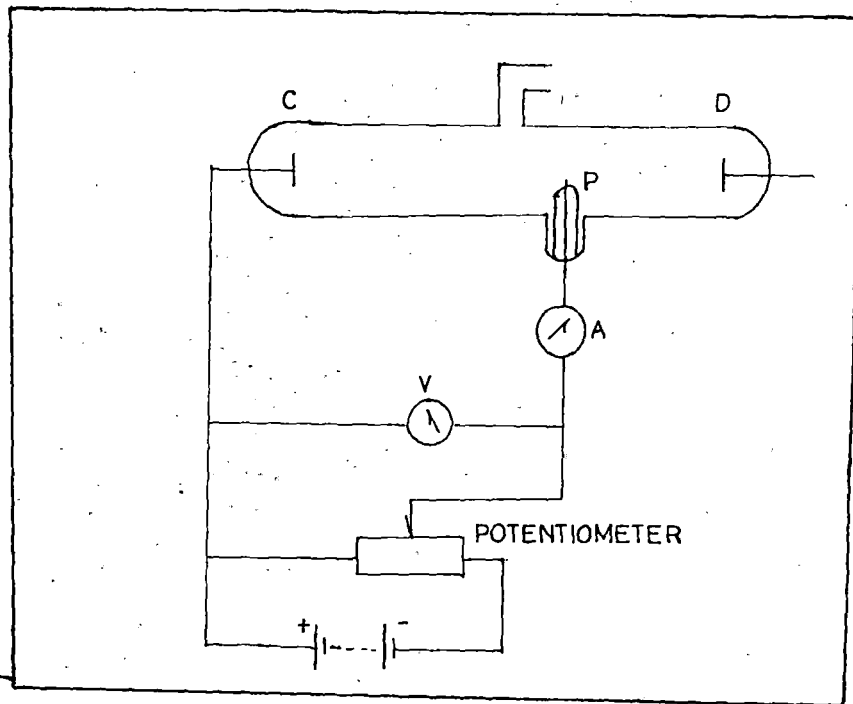


FIG. 213(a) SCHEMATIC EXPERIMENTAL ARRANGEMENT FOR MEASURING ELECTRON TEMPERATURE.

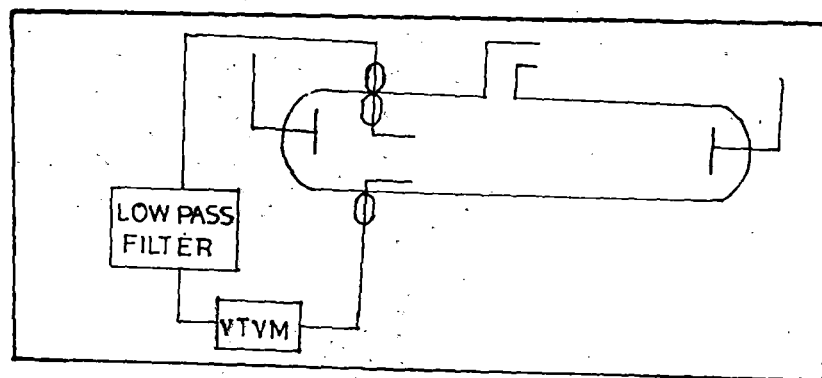


FIG. 213(b) SCHEMATIC EXPERIMENTAL ARRANGEMENT FOR MEASURING DIFFUSION VOLTAGE.

The probe current measurement circuit has been shown in Fig. (2.13,a). The probe was supplied with d.c. bias from dry battery through a potentiometer. For change over from ion current to electron current an external polarity reversal arrangement is necessary to measure the respective current. With the help of bandswitch the operation was made manually. Here probe circuit was connected to anode and the probe potential which is relatively negative with respect to anode was varied in steps of 0.2 - 5 volts. The probe current, which was measured, was total current through the probe. Electron current I_e was determined by subtracting ion current I_i from the total probe current.

$$I_e = I_{tot} + |I_i| \quad (2.5)$$

In fact, in the investigation I_i was smaller than I_{tot} by a factor of order 1000. So effectively I_e equals to I_{tot} .

The details of probe data analysis will be given in chapter VIII.

2.12. Measurement of diffusion voltage by probes.

Two cylindrical probes (tungsten) of length 0.8 cm and radius 0.014 cm were placed parallel to one another one along the axis $r=0$ and the other at a distance of 0.6 cm from the axis in the same cross sectional plane (Fig.2.13,b)

of the arc tube of 41 cm length. The output voltage at the two probes was measured by a V.T.V.M. having an internal impedance of $100\text{ M}\Omega$. A low pass filter circuit was provided at the output of the probes to prevent oscillations generated in the arc from reaching the V.T.V.M. The V.T.V.M. output provides the magnitude of the diffusion voltage. The diffusion voltage has been recorded for a range of arc currents (2A to 5A) and for three back ground air pressures (0.075 torr, 0.10 torr and 0.13 torr).

2.13. Dependence of radial distribution function for the azimuthal conductivity of arc plasma on tube radii

In this diagnostic investigation a radiofrequency coil probe technique has been employed to find the azimuthal radiofrequency conductivity distribution function and its dependence on tube radii. The arc has been created in an arc tube (fig. 2.14) of four different tube radii namely 0.49 cm, 0.78 cm, 0.875 cm and 1.185 cm. Besides the two tungsten mercury pool electrodes at the two ends, two tungsten probes have been inserted upto the axis of the tube in the positive column region with a separation 8.5 cm/8.5 cm/6.6 cm/9.3 cm between them. As shown in the Fig. (2.14); a small coil of length 9.0 cm/5.6 cm/5.9 cm/4.0 cm has been wound around the tube in the respective region of probe-to-probe separation. These coils provide radiofrequency power

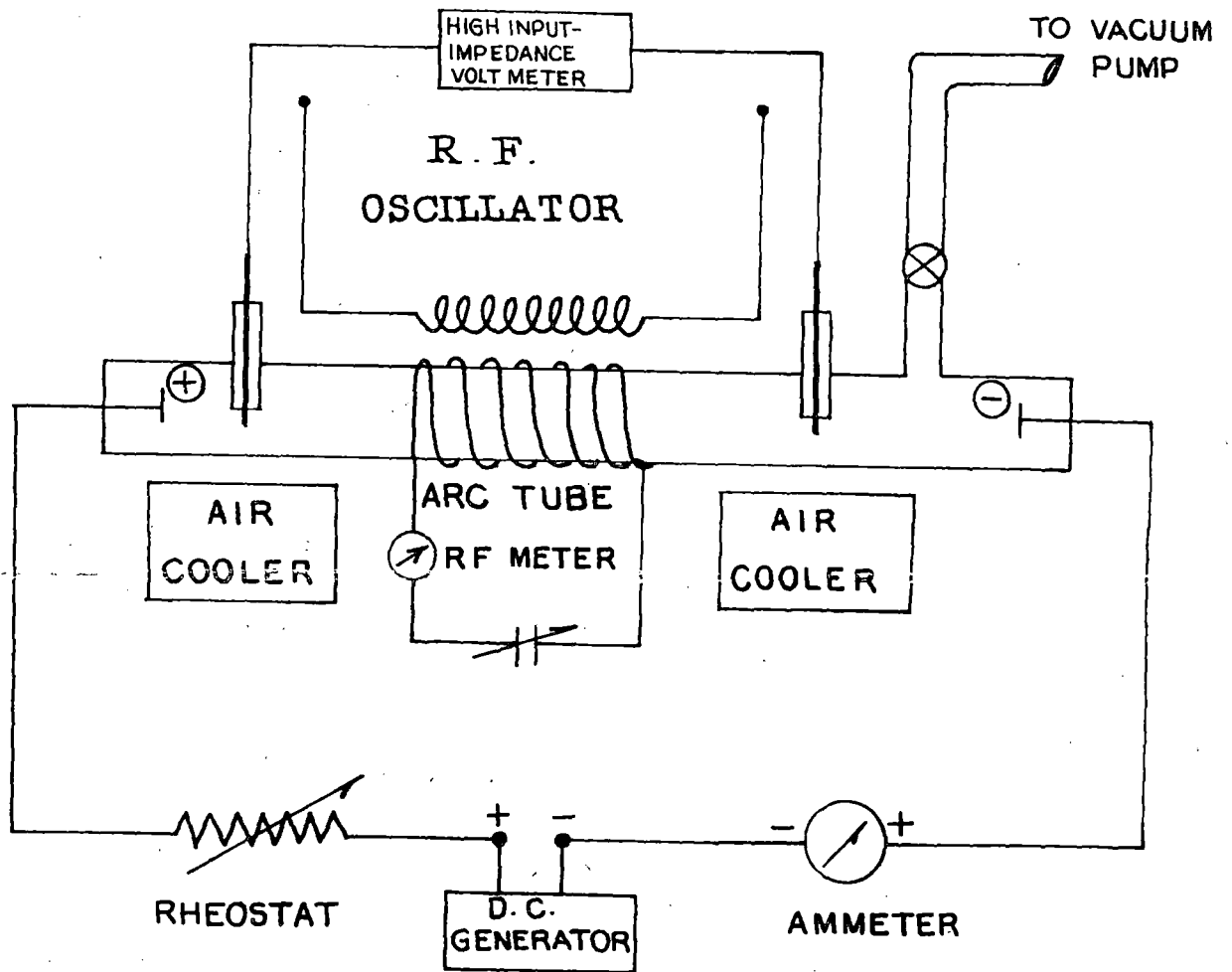


Fig. 2-14. Schematic Experimental Arrangement :
 Distribution function for the dependence of radial
 Azimuthal conductivity of arc plasma on tube Radii.

induction from the externally used high frequency oscillator, input power in which has been provided from a d.c. stabilised high voltage power supply. A radiofrequency milliammeter ranging from 0 - 120 mA (Thermocouple type, made by Weston Instruments, Inc, USA Model No. 308) in series with a gang condenser kept for tuning has been connected at the two leads of the coil wound around the arc tube. These three elements connected in series act as a secondary tank circuit in the investigation (Fig. 2.14) (The detailed theoretical calculation (Ghosal, Nandi, and Sen, 1976, 1978) has been given in review article).

The oscillator coil is placed near the work coil i.e. the coil is wound surrounding the arc tube; and the induced r.f. voltage is tuned with the variable condenser (which is provided with graduated dial scale in degree) inserted in the secondary circuit in series with the r.f. milliammeter and the work coil. Arc is then generated within the tube by following the tilting process. Subsequently the r.f. meter indicator shifts from its previous position. The tuning condition is made by the variable gang condenser. A number of air coolers and a water circulation system have been provided for cooling the arc and to maintain a steady wall temperature. The r.f. meter reading is then noted as far accurately as possible. This current reading is i_1 . Now without disturbing any element of the circuit, the arc is switched off. The meter reading indicator again shifts from

its previous position. The tuning condition is again made by the condenser and the tuned current i_0 is recorded. The voltage across the two probes stuck in the positive column has been noted with help of an electronic multimeter with high input impedance.

It is noteworthy that once the arc is produced and the arc tube placed and the secondary tuned, extreme precautions have been taken so that no element of the associated circuit and their relative positions are disturbed any more till one set of observations is completed. Very good care and caution has also been taken during the whole process of observation such that any mercury droplet could not appear inside the tube in the wound coil region, the presence of which changes the subsequent reading a lot. The observation has been carried out for a fixed oscillator frequency, 3.69 MHz. In this way, for different discharge currents, α , the ratio of tuned radiofrequency current in the absence and in presence of the discharge was measured in an arc tube. Now taking another tube of different radius the whole observation has been made. In the investigation four arc tubes of different radii have been taken to observe the dependence of α and hence the distribution function on tube radii.

2.14. Tube specification and circuit constants

Parameter	Set I	Set II	Set III	Set IV
Outer diameter of the tube in cm	1.22	1.83	2.15	2.64
Inner diameter of the tube in cm	0.98	1.56	1.75	2.35
Coil length in cm	9.0	5.6	5.9	4.0
Coil diameter in cm	1.22	1.83	2.15	2.64
Wire diameter in cm	0.2	0.2	0.2	0.2
Probe-to-probe separation in cm	8.5	8.5	6.6	9.3
No. of turns	77	44	50	33
Inductance in μH	10	10	19	16
Radiofrequency resistance in Ω	14	11	19	15

2.15 R.F. oscillator circuit

The radiofrequency oscillator is of Hartley type; and the circuit diagram is shown in the fig. (2.15,a). It has been designed to cover a range of 3.3 MHz to 10.1 MHz. The inductance L of the tank circuit is divided into two parts L_1 and L_2 and their common point is connected to the cathode terminal of the vacuum tube 811. The end of L_1 is connected to the grid through the parallel combination of R_g

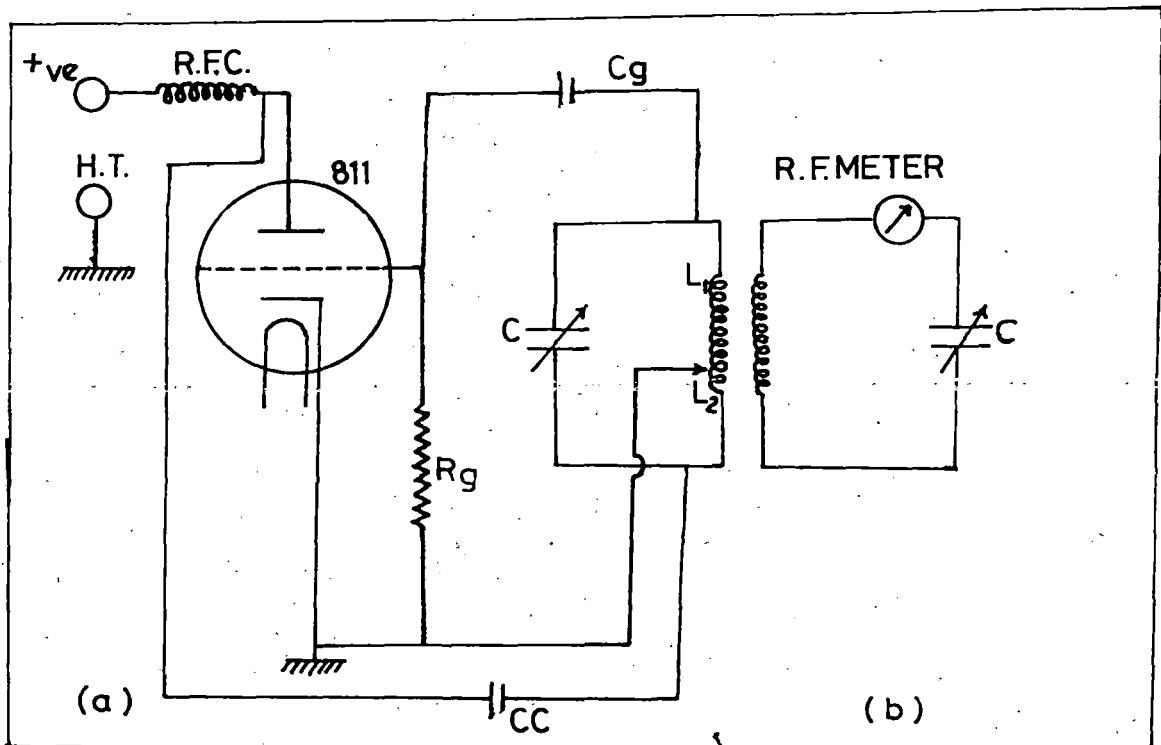


FIG.2:15. RADIO FREQUENCY OSCILLATOR CIRCUIT-(a); SECONDARY TUNING CIRCUIT-(b).

and C_g , which provides the grid bias potential. The end of L_2 is connected to the plate of the oscillator valve 811 through the blocking capacitor C_c . Another variable gang condenser is inserted in parallel with the inductance (primary coil), thereby making a complete tank circuit. The current circulating in the resonant circuit passes through both parts of the inductance and develops a potential difference for the grid excitation. The direct component of the plate current is supplied from a stabilised high voltage power supply through a radiofrequency choke. The blocking capacitor C_c , which has a small reactance compared with the load impedance, gives a path to the a.c. component, while the d.c. from the power supply is prevented. For a fixed gang condenser position, the oscillator frequency (3.69 MHz) has been measured in the experiment by an absorption wavemeter. The secondary receiving circuit, as discussed earlier, consists of the coil wound around the arc tube, a variable tuning condenser and a radiofrequency milliammeter (all connected in series, Fig. (2.15,b)). The dials of the condenser in the secondary (receiver) circuit have been calibrated in terms of capacitance with the help of an L.C.R. Bridge (Model No. 921) and also by Q meter (RADART Type 5902). The dial readings against capacitance are shown in Fig. 2.16.

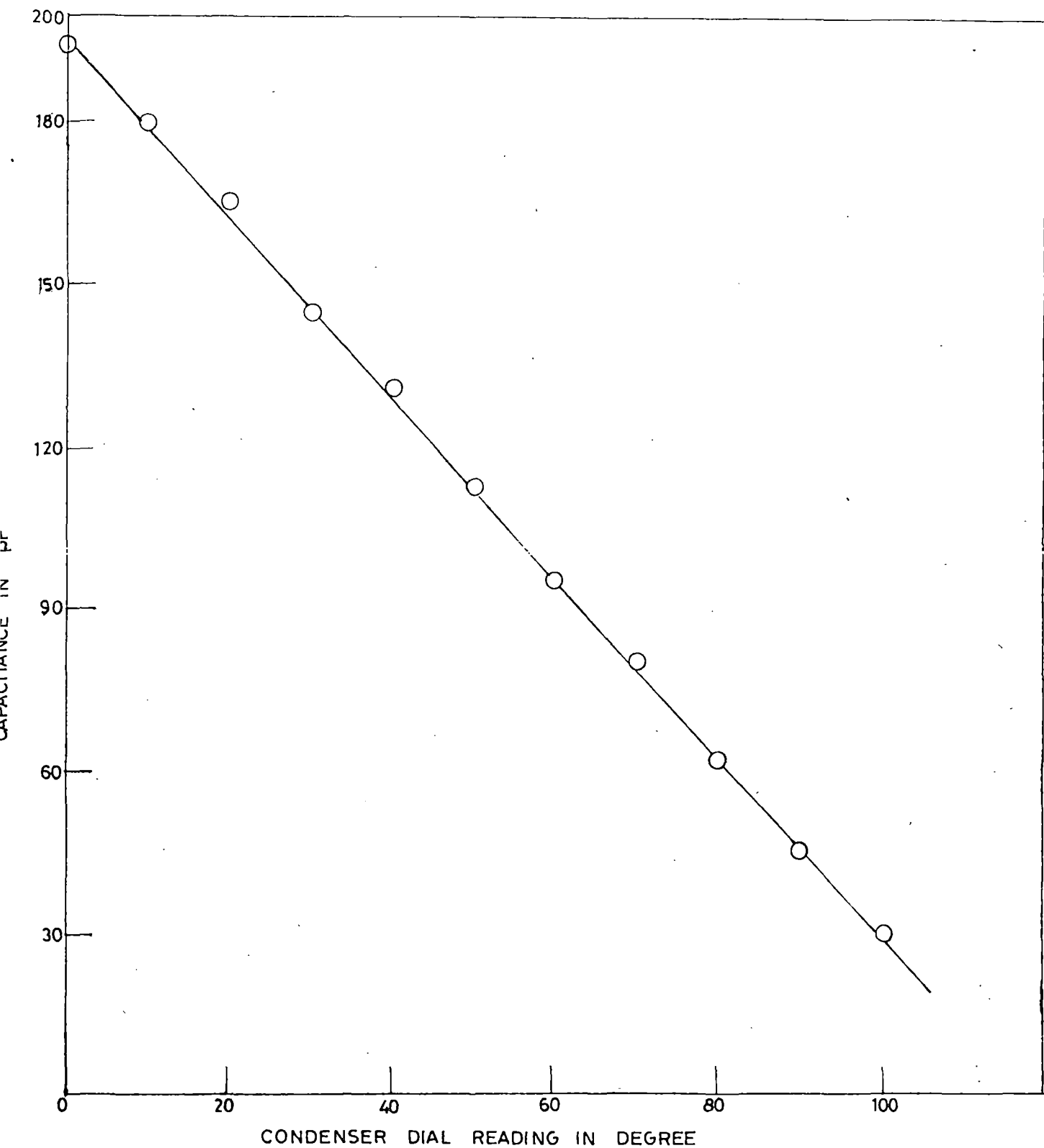


FIG.2:16.CALIBRATION OF THE VARIABLE TUNING CONDENSER IN THE RECEIVER CIRCUIT.

Table 2.1

Dial calibration of the variable tuning condenser in the receiver circuit.

Dial reading in degree	Capacitance in pF	Dial reading in degree	Capacitance in pF
00	195	50	112
10	180	60	95
20	165	70	80
30	145	80	62
40	130	90	45
		100	30

2.15. Measurement of inductance L and mutual inductance M .

With the help of L.C.R. bridge (Model No. 921) and 'Q' Meter (RADART Type 5902) the inductance of work coil has been measured at the working frequency of r.f. signal (3.69 MHz). The value of inductance obtained is to a small extent in error by the presence of the self capacity of the coil. But in the experiment the true L has been measured at the frequency concerned.

After calculating the value of L , the value of the mutual inductance M has been estimated considering plasma inductance to be a secondary with unit turn (Simpson, 1960).

2.16. Measurement of Radiofrequency Resistance (R_o) of the secondary tuning circuit.

The procedure utilised here for estimating the radiofrequency resistance of the coil surrounding the arc tube may be designated as reactance variation procedure. The coil consists of an inductance (the coil wound around the positive column) variable condenser and a radiofrequency milliammeter connected in series. The coil is loosely coupled to the radiofrequency oscillator (Hartley type), and is then tuned to the desired frequency (in the experiment 3.69 MHz) of the driving oscillator by rotating the gang condenser knob. The resonant current I_o in the r.f. milliammeter and the value of the capacitance of the tuning condenser (C_o) are noted. Then the value of the capacitance in the condenser is changed by δC_1 , so that the current (I_1) in the r.f. meter becomes 1/2 times of the resonant current I_o . C_o is again changed by δC_2 in the opposite direction so that the current in the r.f. meter becomes again equal to I_1 .

It can be then be shown that

$$R_o = \frac{1}{155} \frac{\Delta C}{C_o^2} \lambda \quad (2.4)$$

where R_o is the radiofrequency resistance in Ω

$$\Delta C = \delta C_1 + \delta C_2 \quad \text{in Farad}$$

λ = wave length of r.f. voltage. Hence R_o has been estimated.

1. Cobine, J.D. (1958), Gaseous Conductors: theory and engineering applications (Dover Publication, New York).
2. Hodgman, C.D. (1956), Handbook of Chemistry and Physics, 38th. Edn. (Chemical Rubber Publishing, Co., Ohio).
3. International Critical Tables of Numerical Data (1926), vol.5, (McGraw Hill Book Co., N.Y.).
4. Lamar, E.S. and Compton, K.T. (1931), Phys. Rev., 37, 1069.
5. Radio Amateur's Hand Book (1965), 42nd. Edn. (American radio relay league, West Hartford).
6. Simpson, P.G. (1960), Induction Heating (McGraw Hill Book Co., Inc.).
7. Verweij, W. (1960), Philips Res. Rep. Suppl. No. 2.